Developmental and Comparative Immunology 88 (2018) 55–64

Contents lists available at ScienceDirect

Developmental and Comparative Immunology

journal homepage: www.elsevier.com/locate/devcompimm

Establishment of fin cell lines and their use to study the immune gene expression in cyprinid fishes with different ploidy in rhabdovirus infection

Jun Xiao[1], Yongming Fu[1], Wei Zhou, Lingzhi Peng, Jun Xiao, Shaojun Liu, Hao Feng*

State Key Laboratory of Developmental Biology of Freshwater Fish, College of Life Science, Hunan Normal University, Changsha, 410081, China

ARTICLE INFO

Keywords:
Innate immunity
Ploidy
Fish cell line
SVCV
Transcriptome

ABSTRACT

Triploid hybrid (3n = 150) of red crucian carp (♀, 2n = 100) and allotetraploid (♂, 4n = 200) display improved disease resistance and stress resistance than their parents. In order to elucidate their innate immune mechanisms, three novel cell lines from the caudal fin of red crucian carp, triploid hybrid and allotetraploid (named 2nFC, 3nFC and 4nFC accordingly) were established and characterized respectively. 2nFC, 3nFC and 4nFC showed fibroblast-like morphology and characteristics. They have been subcultured for more than 100 passages since the initial primary culture. Viral infection experiments showed that 2nFC, 3nFC and 4nFC were susceptible to spring viraemia of carp virus (SVCV) infection. Intriguingly, 3nFC performed the stronger resistance ability against SVCV than 2nFC and 4nFC, which indicated that 2nFC, 3nFC and 4nFC might be used as the suitable *in vitro* models for exploring and analyzing the differences among these three cyprinid fishes in antiviral innate immune mechanisms. Based on this, we analyzed the transcriptome profile of 2nFC, 3nFC and 4nFC in the context of SVCV infection. The KEGG enrichment analysis showed that the differentially expressed genes (DEGs) were primarily enriched to immune-related signaling pathways. However, some signaling pathways against viral infection were activated remarkably in 2nFC and 3nFC but not in 4nFC. Overall, the establishment of 2nFC, 3nFC and 4nFC provided us a suitable platform to elucidate the innate immunity of fishes with different ploidy and clear genetic relationship.

1. Introduction

Polyploidization exists in vertebrates and plants, however, it happens more frequently in plants (Mable, 2004, 2013). Polyploidization in vertebrates seldom shows positive effects and more often results in lethal consequences because viable gametes fail to form during meiosis (Liu et al., 2016). Fortunately, allotetraploid (AT; 4n = 200) has been developed by crossing red crucian carp (*Carassius auratus*red var., ♀, 2n = 100) with common carp (*Cyprinus carpio* L., ♂, 2n = 100) and subsequently selective breeding. Both male and female individuals of allotetraploid are fertile and this allotetraploid population has propagated 26 generations (Liu et al., 2001). Triploid hybrid (3n = 150) was developed through the hybridization between the male allotetraploid and the female diploid red crucian carp (Chen et al., 2009; Liu et al., 2004; Shen et al., 2006). Triploid hybrid possesses many merits, such as fast growing and good taste, which make it an economic important species in Chinese fresh water aquacultural industry (Liu, 2010). Especially, triploid hybrid displays much improved disease resistance and stress resistance than its parents (Liu, 2010). As to these three fish species with different ploidy and clear genetic relationship, extensive studies had been conducted to explore their development, reproduction and physiology, however, there were few reports about the immunity of these fish species (Duan et al., 2016; Long et al., 2006; Zhang et al., 2005).

Cell lines are valuable *in vitro* models to study virology, pathology, developmental biology and immunology of both lower and higher vertebrates (Lakra et al., 2011; Zhang et al., 2003). Up to now, a lot of fish cell lines have been established from different fish species, such as zebrafish (*Danio rerio*), rainbow trout (*Oncorhynchus mykiss*), crucian carp (*Carassius auratus*), grass carp (*Ctenopharyngodon idella*), orange spotted grouper (*Epinephelus coioides*), black carp (*Mylopharyngodon piceus*) etc (Driever, 1993; Luque et al., 2014; Qin et al., 2006; Xue et al., 2018; Zhang and Gui, 2004; Zuo et al., 1986). Many studies reported that fish fibroblasts were able to express abundant cytokines and immune-related receptors, which suggested that fibroblasts might play an important role in both the innate and adaptive immunity in fish (Ingerslev et al., 2010; Villena, 2003). Allotetraploid, diploid red crucian carp and their triploid hybrid offspring offer a unique system for

* Corresponding author.
E-mail address: fenghao@hunnu.edu.cn (H. Feng).
[1] These authors contribute equally to this paper.

https://doi.org/10.1016/j.dci.2018.07.007
Received 8 February 2018; Received in revised form 7 July 2018; Accepted 7 July 2018
Available online 12 July 2018
0145-305X/

the study of the evolution of the innate immunity with several advantages. For example, their known parentage separates them from natural polyploids, and it is easy to trace the fate of progenitor genes (Liu et al., 2016). However, for the studies on the innate immunity, there is a lack of species-specific cell lines of fishes with different ploidy, because they are non-model animals.

In this study, we have established and characterized three cell lines from the primary culture of the caudal fins of diploid red crucian carp, triploid hybrid and allotetraploid separately. These three cell lines were designated as 2nFC, 3nFC and 4nFC accordingly and they showed fibroblast-like morphology. Two marker genes for epidermis (containing epithelial cells) and dermis (containing fibroblasts) were investigated to further determine the cell types of 2nFC, 3nFC and 4nFC. In natural and aquacultural condition, red crucian carp, triploid hybrid and tetraploid fish are facing many pathogenic microbes, such as spring viraemia of carp virus (SVCV) (Yan et al., 2016). Therefore, the susceptibility of 2nFC, 3nFC and 4nFC to SVCV was examined in the current study. At the same time, some antiviral genes like IFNa, PKR, Viperin and Mx1, which induced by fish rhabdoviruses were investigated by qPCR method. Next-generation sequencing (NGS) technologies have provided a new approach for exploring the whole genome and transcriptome information involved in fish immunity in recent years (Morozova and Marra, 2008). By sequencing RNA from infected and uninfected samples, it is possible to identify immune-related genes which are differentially expressed and further lead to a better understanding of molecular mechanisms underlying the host immune response to pathogenic stimuli (Petit et al., 2017). Therefore, we employed RNA-seq technology to investigate the transcriptome of 2nFC, 3nFC and 4nFC in the context of SVCV infection. Overall, the establishment of 2nFC, 3nFC and 4nFC constituted a suitable platform to study the immune gene expression in cyprinid fishes with different ploidy in rhabdovirus infection.

2. Materials and methods

2.1. Primary cell culture and subculture

Healthy red crucian carp (6 g in weight), triploid hybrid (19.8 g in weight) and allotetraploid (146 g in weight) were collected from the Engineering Research Center of Polyploid Fish Breeding and Reproduction of State Education Ministry in Hunan Normal University. After thoroughly removing the surface mucus on the body of the fish, the caudal fins were clipped, disinfected with 75% ethanol and washed with phosphate-buffered saline (PBS) containing 200 U/ml penicillin and 200 μg/ml streptomycin (HyClone). Thereafter, the fins were minced into pieces (approximately 1 mm^3) by using sterile scissors and then placed in fetal bovine serum (FBS; Gibco). Tissue pieces were seeded into 8-cm^2 dishes and incubated at 26 °C with 5% CO2 equilibrium. After 1 h, 3 ml DMEM (Gibco) with 30% FBS and 20 ng/ml bFGF (Sigma) was added to the dishes.

Fifty percent of the media was changed every 3–5 days with fresh DMEM supplement with 30% FBS, 20 ng/ml bFGF, 100 U/ml penicillin and 100 μg/ml streptomycin. Subculture was carried out at a split ratio of 1:2 subsequently by trypsinization when primary cell cultures grew to 90–100% of confluence. After 15 passages, the concentration of FBS in the medium was decreased from 30 to 15%, and the bFGF was decreased to 10 ng/ml.

2.2. Cell growth and cell transfection

Growth characteristics of 2nFC, 3nFC and 4nFC were evaluated by cell doubling-time assay. Cells at a density of 2.0×10^5 cell/well were seeded into 6-well plates and incubated at 26 °C. Every other day, cells were trypsinized and collected for hemocytometric determination of cell number. All experiments were undertaken in triplicate.

2nFC, 3nFC and 4nFC were seeded into 6-well plates at a density of 2×10^5 cell/well separately. After being cultured for 24 h, cells were transfected with pEGFP-N1 by using LipoMax (SUDGEN), Lipofectamine®2000 (Invitrogen) or calcium phosphate according to the manufacturer's instruction respectively (Liu et al., 2017). Green fluorescence signals were detected by fluorescence microscope, and the transfection efficiency was determined by counting green fluorescent protein-positive and total cells from 20 random fields at 48 h post transfection.

2.3. Chromosomal analysis and flow cytometry

Chromosomal analyses of the 2nFC, 3nFC and 4nFC were performed at passage 50. Exponentially growing cells in 10-cm dishes were treated with colcemid (0.1 mg/ml) for 3 h. The cells were harvested and followed by hypotonic treatment with 0.075 M KCl at 26 °C for 25–30 min, then fixed in methanol-acetic acid (3:1, v/v) with three changes. Then cells were stained according to a previously described method (Xiao et al., 2014). Chromosome metaphases were observed and photographed with Pixera Pro 600ES (US). For each cell line, 100 good-quality metaphase spreads were analyzed.

Cells in 10-cm dishes were collected and washed three times with PBS. The cells were re-suspended in pre-cooling ethanol and fixed overnight at 4 °C. The fixed cells were washed three times with PBS and re-suspended in PBS at a concentration of 1×10^6 cells/ml. PI (50 μg/ml) and RNase A (20 μg/ml) were added into the cell suspension to stain the cells in the dark for 30 min. After PI staining, the cells were analyzed with flow cytometer for the DNA content measurement.

2.4. Virus production and infection

The strain 741 of SVCV (SVCV-741) was kindly provided by Dr. Yong' an Zhang (Institute of Hydrobiology, CAS). The virus was propagated in EPC cells at 25 °C in the presence of 2% FBS. Virus titer was determined by plaque assay in EPC cells as previously described (Xiao et al., 2017). Briefly, the 10-fold serially diluted virus supernatants were added onto EPC cells and incubated for 2 h at 25 °C. The supernatant was removed after incubation and DMEM containing 2% FBS and 0.75% methyl cellulose (Sigma) was added. Plaques were counted at day-3 post infection.

For viral infection, 2nFC, 3nFC or 4nFC were seeded into 12-well plates at 1×10^5 cells/well at 26 °C for 24 h. SVCV were added into the culture media at the dose of 0.003, 0.03, 0.3 or 3 MOI, respectively. After 1 h incubation, the media containing viruses was replaced with fresh media after washing twice with DMEM. Anther 24 h later, the supernatants were collected for viral titer measurement using plaque assay as previously described (Wu et al., 2017).

2.5. RNA-seq samples collection

2nFC, 3nFC and 4nFC were separately propagated in 10-cm dishes at 26 °C. When the cells were 100% confluent, the cells were infected with SVCV at MOI of 3×10^{-3} while the control cells were only exposed to the DMEM growth media. After 1 h incubation, the virus containing media was replaced with fresh DMEM (2% FBS) after washing twice with DMEM. Thereafter, the SVCV infected and non-infected cells were incubated at 26 °C for 36 h and harvested for RNA extraction respectively.

2.6. RNA extraction, sequencing, de novo assembly and annotation

Total RNA isolation was performed by following the instruction of the TRIzol reagent product manual (Invitrogen). Then RNA was treated with DNase I to remove any genomic DNA traces. The concentration and quality of RNA was examined through NanoDrop and agarose gel electrophoresis. Double-stranded cDNA was synthesized from mRNA. cDNA library preparation and sequencing reactions were conducted

using Illumina HiSeq™ 2500 platform by OE Biotech Co. Ltd. (Shanghai, China).

Clean reads were obtained after removal of adaptor sequences and low quality reads. The *de novo* assembly of RNA-seq was performed by using Trinity software. Thereafter, by using the BlastX alignment (cut-off E-value of 10^{-5}), the assembled unigenes were annotated into different functional classifications after searching in different public databases, including NCBI non-redundant protein sequences (Nr), Swiss-Prot (a manually annotated and reviewed protein sequence database), Clusters of orthologous groups for eukaryotic complete genomes (KOG), Kyoto Encyclopedia of Genes and Genomes (KEGG) and Gene Ontology (GO). Blast2GO software was used to obtain Gene Ontology (GO) (http://www.geneontology.org/) annotation of the unigenes based on BlastX hits against the Nr database (E-value < 10^{-5}). Each annotated sequence was assigned to detailed GO terms and calculated under categories of biological process, cellular component and molecular function. The unigene sequences were annotated in Swiss-Prot database using the BlastX (E-value < 10^{-5}). The unigene sequences were also aligned to the KOG database (ftp://ftp.ncbi.nih.gov/pub/COG/KOG/kyva) to predict and classify functions. Pathway assignments were generated using the KEGG database (http://www.genome.jp/kegg/pathway.html) and the BlastX algorithm with an E-value threshold of 10^{-5}.

2.7. Differential gene expression analysis

Gene expression levels were calculated using the fragments per kilobases per million mapped reads (FPKM) method. The identification of differentially expressed genes (DEGs) between control group and SVCV infection group was performed using the DESeq packages (DEGs of 2nFC, 3nFC and 4nFin samples were separately screened). Only the DEGs with a threshold of p-value < 0.05 and $|\log_2(\text{fold change})| > 1$ were considered differentially expressed. For the identification of the pathways that the DEGs are predicted to participate in, all DEGs were mapped to terms in the KEGG databases and searched for significantly enriched KEGG terms.

2.8. Quantitative real-time PCR (q-PCR) verification

Quantitative real-time PCR (qPCR) was used to detect the gene transcription levels for immune-related genes. Specific primers were designed with Primer5 software based on the target sequences. The primers used for qPCR of the selected DEGs are listed in Table 1. The qPCR reaction was prepared in a real-time PCR plate, using SYBR green as the fluorescent reagent and an ABI 7500 fast real-time PCR system. The program of q-PCR was: 1 cycle of 50 °C/2min, 1 cycle of 95 °C/10min, 40 cycles of 95 °C/15s, 60 °C/1min, followed by dissociation curve analysis (60 °C −95 °C) to verify the amplification of a single product. The threshold cycle (CT) value was determined by using the manual setting on the 7500 Real-Time PCR System and exported into a Microsoft Excel Sheet for subsequent data analyses where the relative expression ratios of target gene in treated group versus those in control group were calculated by $2^{-\triangle\triangle CT}$ method. Negative controls with no reverse transcriptase were performed in all the experiments.

3. Results

3.1. Establishment and characteristic of 2nFC, 3nFC and 4nFC

The primary cells were initiated from caudal fin of red crucian carp, triploid hybrid or allotetraploid fish separately. The fibroblast-like cells migrated from the tissue fragments and formed a monolayer within 6–14 days. Then, the fibroblast-like cells (2nFC, 3nFC and 4nFC) were incubated at 26 °C and subcultured over 100 times (Fig. 1A). As for fin cells, two dominant cellular types are reported: fibroblasts and epithelial cells (Mauger et al., 2009) because fin cells are mainly from epithelial and fibroblastic origin. To characterize the cell types of 2nFC, 3nFC and 4nFC, we investigated the marker genes which expected to be differentially expressed in epidermal (*cytokeratin 49*, *ck49*) and dermal (*type I collagen isoform a1*, *col1a1*) cells (Chenais et al., 2015; Mauger et al., 2009). The results showed that the *col1a1* mRNA relative abundance was very high. Conversely, the relative abundance of *ck49* in 2nFC, 3nFC and 4nFC is very low (Fig. 1B), which suggested that these three cell lines are majorly composed of fibroblast cells. 2nFC, 3nFC and 4nFC cells at passage 50 were analyzed for cell growth kinetics separately, in which the doubling time of 2nFC, 3nFC and 4nFC were 36.6 h, 38.9 h and 41.3 h, respectively (Fig. 1C). To see if these fibroblast cells were good models for immunological study, 2nFC, 3nFC and 4nFC were transfected with pEGFP-N1 plasmid by using different methods separately and used for fluorescence microscope, in which the highest EGFP expression was observed in the cells transfected through LipoMax method (Fig. 1D).

Table 1
Primers used for qPCR (all primer sets are checked to be completely identical to the sequences of target genes of both red crucian carp and common carp).

Primer name	Primer sequence 5'-3'	Annealing temperature (°C)
RIG-I-F	GGAAGAATACCACAATAAC	53.0
RIG-I-R	TCCAATCAGGACTCCAGGC	55.3
MAVS-F	GTAACTGTGAACATTGGG	50.3
MAVS-R	GAAGTATAAGAAGGAGCC	50.3
TBK1-F	CTGAAAAAACTCAACCAC	48.1
TBK1-R	CTTCCACACGGACAATAC	52.6
IRF7-F	CCCAACAAATCATTCCG	50.2
IRF7-R	AGGTTACATTGCTGCCC	52.2
TRAF6-F	GCAGTATCAAGGCGTC	51.7
TRAF6-R	CGTGTAGAAAGGTGGG	51.7
IFNa-F	GAGGACCAGGTGAGGT	54.3
IFNa-R	GATGACTGCCKYTGC	50.4
PKR-F	CRGCAGRCAGGTGATG	51.7
PKR-R	CCCTTTAGTCCGTTCC	51.7
Viperin-F	CGAGGCTTACGACTT	48.4
Viperin-R	GAACCAGGTTTCTSTG	48.9
Mx1-F	CACGCACATCATCTTT	50.1
Mx1-R	TTTATCCGCAACACTA	50.2
SVCV-N-F	GGATTCAGGGGGATAAGA	52.6
SVCV-N-R	ACCCAGCAAGAAGAGAGG	54.9
β-actin-F	TGGGCACCGCTGCTTCCT	59.5
β-actin-R	TGTCCGTCAGGCAGCTCAT	57.3
ck49-F	AGCGTCAACGGCAAGAGTAT	55.4
ck49-R	TGAGGATGAGGATGAGGATTG	55.6
col1a1-F	CCGATGATGCCAATGTG	52.2
col1a1-R	GGTCAGGGTCAATCCAGTA	55.2

3.2. Cytogenetical analysis of 2nFC, 3nFC and 4nFC

The previous study had verified that the chromosome numbers of red crucian carp, triploid hybrid and allotetraploid fish are 100, 150 and 200, respectively (Zhang et al., 2005). To determine the chromosome numbers of 2nFC, 3nFC and 4nFC, 100 metaphase plates of each cell line (at passage 50) were examined respectively. The results showed that the chromosome numbers of 2nFC ranged from 90 to 100, and the modal number was 92 (Fig. 2A); the chromosome numbers of 3nFC ranged from 120 to 148, with a distinct peak at 136 (Fig. 2B); the chromosome numbers of 4nFC ranged from 150 to 200, with a modal number of 172 (Fig. 2C). The typical metaphase of 2nFC (92), 3nFC (136) and 4nFC (172) were shown in Fig. 2D, E and F accordingly. Flow cytometry was employed to further examine the DNA content of these cells, which showed that the relative DNA content of these cells correlated with the chromosome numbers of these cells. The mean DNA content of 3nFC was around 1.5 times as high as that of 2nFC, and the mean DNA content of 4nFC was also around 2 times against that of 2nFC (Fig. 2G ~ I). Combining the data of chromosome number and DNA content, it was speculated that there existed chromosome losing

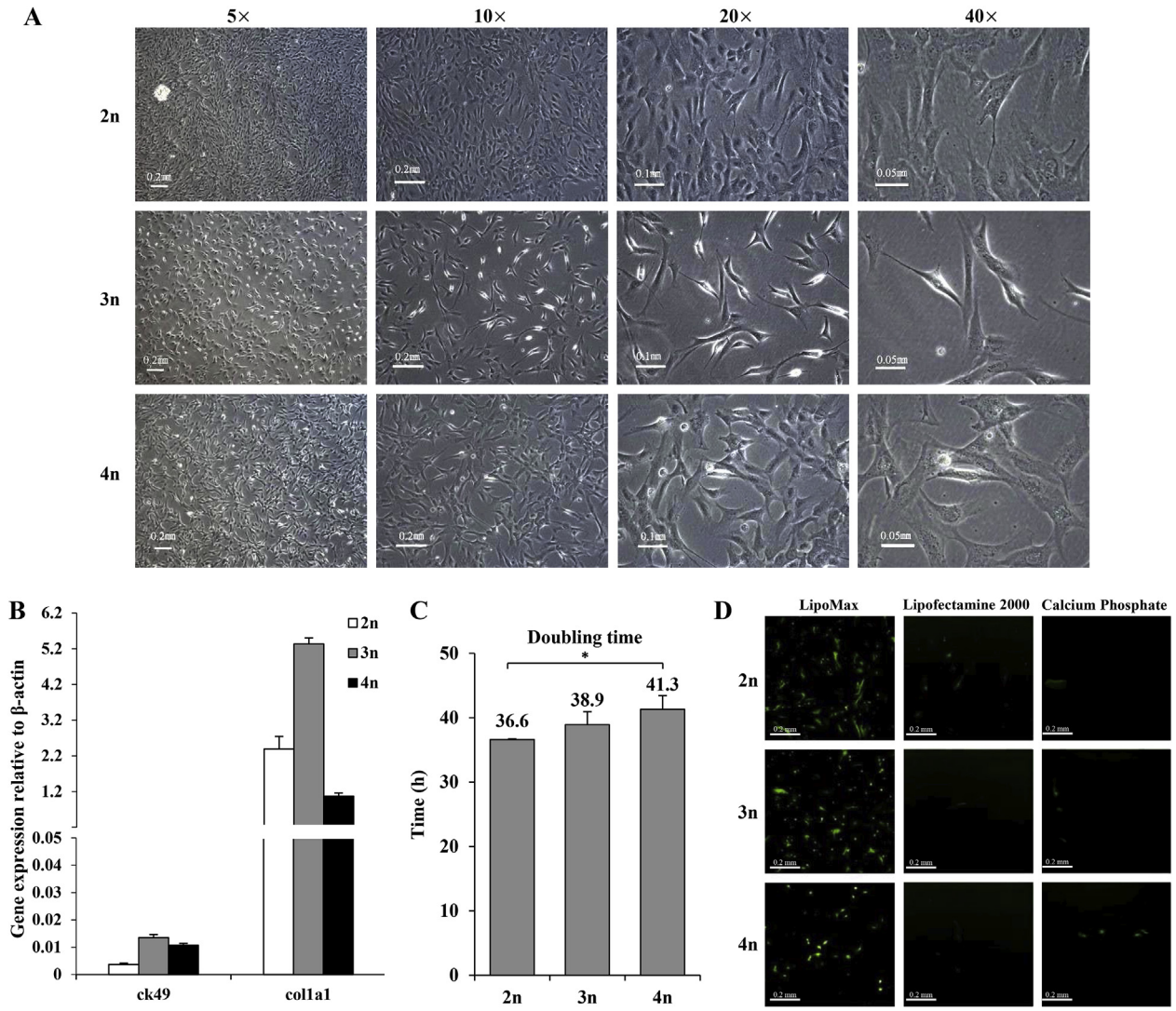

Fig. 1. Establishment and characteristic of 2nFC, 3nFC and 4nFC. **(A)** Fibroblast-like morphology of 2nFC, 3nFC and 4nFC at passage 50 after primary culture in 5 ×, 10 ×, 20 × and 40 × magnification, respectively; **(B)** qPCR detection of the transcript level of *ck49* and *col1a1* in 2nFC, 3nFC and 4nFC. Data are shown as the mean gene expression relative to the expression of endogenous control β-actin. Error bars represent + SD of three independent experiments. **(C)** Doubling time of 2nFC, 3nFC and 4nFC grown in DMEM supplemented with 15% FBS at 26 °C; the numbers stand for the average doubling time of the cells; error bars represent the standard error of the mean (+SEM) of three independent experiments (*$p < 0.05$). **(D)** Transfection of 2nFC, 3nFC and 4nFC. Cells were transfected with pEGFP-N1 separately by the indicated methods. At 48 h post transfection, the cells were subjected to fluorescent micrograph analysis (10 × magnification). 2n:2nFC; 3n:3nFC; 4n:4nFC.

during the cell subculture of these three cell lines.

3.3. The susceptibility of 2nFC, 3nFC and 4nFC to SVCV

To test the susceptibility to SVCV, 2nFC, 3nFC and 4nFC were infected with SVCV at different dose and used for viral titration experiments, respectively. In all infection groups, the viral titer in the supernatant media of the 3nFC was obviously lower than those of 2nFC and 4nFC, especially in the 0.003 MOI group (Fig. 3A). To better characterize the susceptibility of 2nFC, 3nFC and 4nFC to SVCV, we evaluated the cell viability and viral titer of these cell lines at 12 h, 24 h or 36 h post infection at 0.003 MOI (Fig. 3B&C). As shown in Fig. 3B, the survival rate of 2nFC, 3nFC and 4nFC was 75%, 89% and 52% at 36 h post infection accordingly, which was determined by Trypan blue staining test. Obviously, 3nFC exposed to SVCV showed highest survival rate. For 4nFC, cultures exposed to SVCV resulted in highest cell death rate. For the viral titers in the supernatant of 2nFC, 3nFC and 4nFC, there is no significant difference among the three cell lines at the 12 h post infection. However, the viral titers in 3nFC supernatant at 24 h and 36 h points were much lower than those of 2nFC and 4nFC at 24 h and 36 h points (Fig. 3C). To determine the replication of SVCV in the three cell lines, the amount of SVCV N transcripts was examined by qPCR. The expression of N transcript in 4nFC was fiercely increased right after infection. In contrast, the increase of N mRNA level in 3nFC was smaller than those in 2nFC and 4nFC (Fig. 3D).

To further elucidate the innate antiviral response of 2nFC, 3nFC and 4nFC to SVCV, the induction of IFNa by the SVCV infection was analyzed. At early time point (2 h and 4 h), the IFNa mRNA levels in 2nFC, 3nFC and 4nFC were almost not increased. However, at 24 h post infection, the IFNa mRNA levels in 2nFC and 3nFC but not in 4nFC were fiercely elevated (Fig. 3E). Meanwhile, the expression of ISGs (PKR, Viperin and Mx1) was examined, which was induced by type I IFNs (Fig. 3F ~ H). Collaborated with the data of IFNa, the mRNA level of all the selected genes obviously increased in 3nFC at 24 h post infection. Viperin and Mx1 expression were enhanced in 2nFC at 24 h post infection. However, only slight increase of all the selected ISGs in 4nFC was seen at 24 h post infection. These results demonstrated that 3nFC performed strongest resistance to SVCV infection and showed quick and

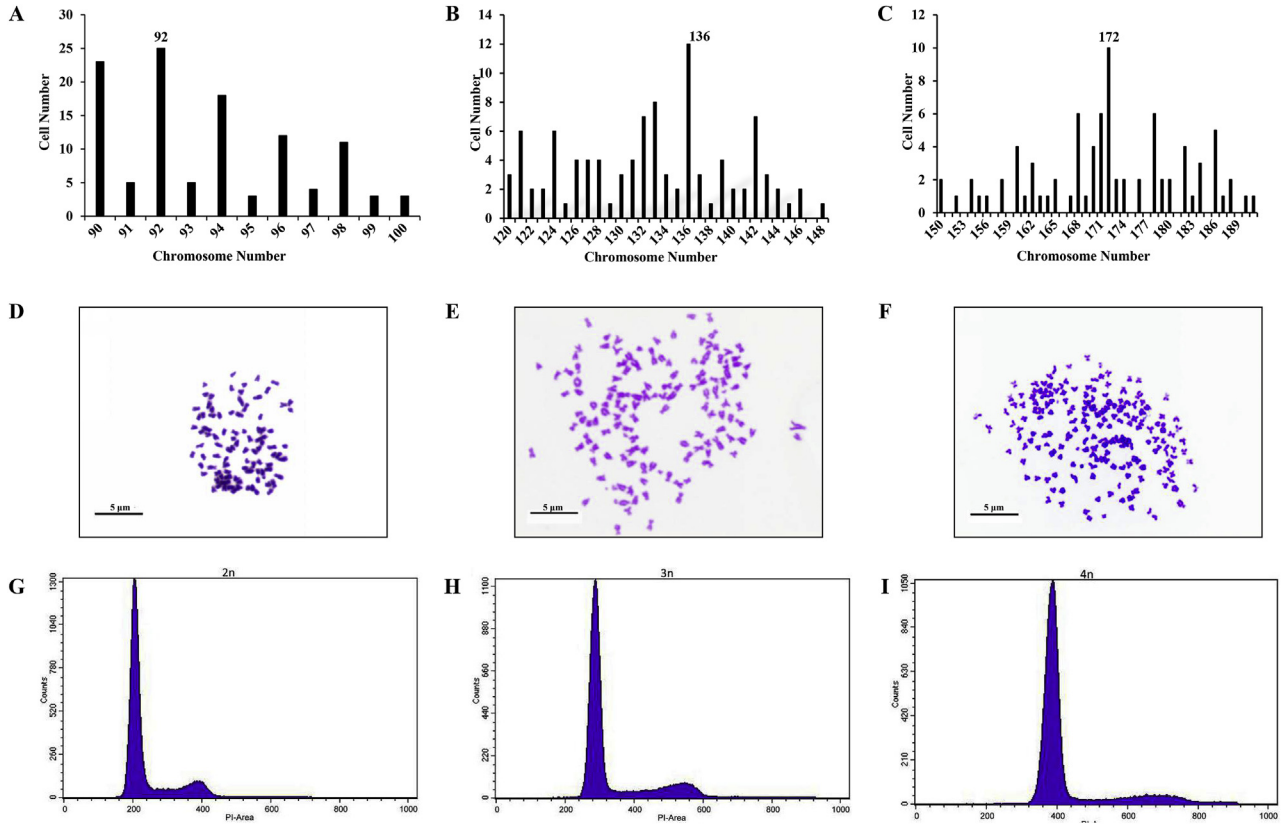

Fig. 2. Chromosome analysis and flow cytometry analysis of 2nFC, 3nFC and 4nFC. **(A–C)** Frequency distribution of chromosomes in 100 cells from 2nFC, 3nFC and 4nFC; **(D–F)** Metaphase chromosome spreads of 2nFC (2n = 92), 3nFC (3n = 136) and 4nFC (4n = 172), the bar stands for the scale of 5 μm; **(G–I)** Cytometric histograms of DNA fluorescence for 2nFC, 3nFC and 4nFC. 2n:2nFC; 3n:3nFC; 4n:4nFC.

strong interferon response to SVCV infection among these three cell lines.

3.4. Sequencing, de novo assembly and functional annotation

To elucidate the mRNA profile of host innate immune related genes in the context of viral infection, the transcriptome of 2nFC, 3nFC and 4nFC in response to SVCV infection were studied, in which 6 cDNA libraries, including the control group (2N CTR, 3N CTR and 4N CTR) and SVCV infection group (2N SVCV, 3N SVCV and 4N SVCV), were constructed and sequenced using the Illumina HiSeq™2500 sequencing platform. Raw sequencing reads were submitted to Sequence Read Archive in NCBI; the SRA accession numbers were SRS2815857, SRS2815853, SRS2815858, SRS2815856, SRS2815854 and SRS2815855. A total of 8.4×10^7, 9.6×10^7 and 9.6×10^7 raw reads were obtained from the 2nFC, 3nFC and 4nFin libraries, respectively. After quality control, data filtering and removing low quality or redundant reads, 41992154, 37219618, 47992506, 25934388, 47992746 and 32388210 clean reads of 2N CTR, 2N SVCV, 3N CTR, 3N SVCV, 4N CTR and 4N SVCV libraries were generated respectively (Table 2). By using *de novo* assembly, 41179, 40547 and 40385 unigenes of 2nFC, 3nFC and 4nFin libraries were separately assembled (Table 3). The mean length of 2nFC unigenes was 1119 bp and N50 was 1936 bp. As for the 3nFC unigenes, the mean length was 891 bp and N50 was 1293 bp. With regard to 4nFC unigenes, the mean length was 976 bp and N50 was 1555 bp. These results indicated that the sequences were high-quality, and the unigenes could be used for further analysis.

To learn genes function information comprehensively, the unigenes of 2nFC, 3nFC and 4nFin were separately annotated by five major databases, including NR, Swiss-prot, KOG, KEGG and GO (Table 4). With regard to the GO enrichment analysis, the unigenes of 2nFC, 3nFC and 4nFC were mainly divided into three categories: cellular component (CC), molecular functions (MF) and biological process (BP). The classification results of the three cell lines showed the same distribution: the most represented terms in CC category were “cell” and “cell part”; the highest represented terms in MF category were “binding” and “catalytic”; the top two terms in BP category were “cellular process” and “metabolic process” (Fig. 4A). Based on KEGG functional classification, we analyzed the unigenes enriched in the immune system-related pathways. It is shown that the immune system-related unigene numbers of 2nFC, 3nFC and 4nFC were similar (Fig. 4B). Collectively, these results indicated that the 2nFC, 3nFC and 4nFC possess abundant biological components related to immune system, which might be used as suitable platform for the study of immunity of diploid red crucian carp, triploid hybrid and allotetraploid fish.

3.5. Analysis of the differentially expressed gene

In order to characterize the gene transcription variation in 2nFC, 3nFC and 4nFC before/after SVCV infection, differential expression analysis was performed. Overall, 2160 DEGs (1485 up-regulated and 675 down-regulated) between 2N SVCV vs 2N CTR, 430 DEGs (386 up-regulated and 44 down-regulated) between 3N SVCV vs 3N CTR, and 1085 DEGs (683 up-regulated and 402 down-regulated) between 4N SVCV vs 4N CTR were identified respectively (Table 5). Then the DEGs were further aligned against the KEGG database for gene function analysis. Top 20 statistics of pathway enrichment in 2nFC, 3nFC and 4nFC were analyzed respectively (Fig.5A ~ C). The data showed that most of them were immune-relate and disease-related pathways. These pathway statistics provided the basic view about the analysis of the genes involved in immune response.

The innate immune system serve as the first line of the host defense

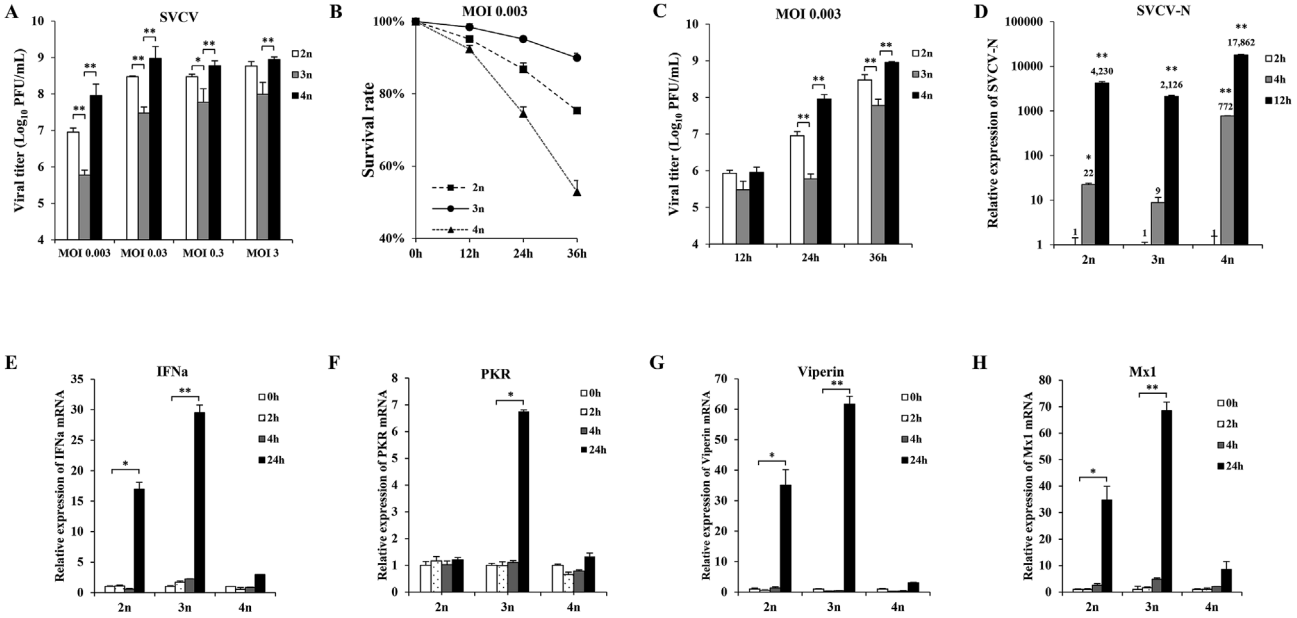

Fig. 3. The susceptibility and IFN/ISGs induction of 2nFC, 3nFC and 4nFC to SVCV. **(A)** 2nFC, 3nFC and 4nFC seeded in 12-well plates were infected with SVCV at indicated MOIs and the culture supernatants were collected at 24 h post-infection. The viral titers of the collected culture supernatants were determined by plaque assays. Data represent mean + SEM (n = 3) and were tested for statistical significance using a one-way ANOVA followed by a Tukey test (*p < 0.05; **p < 0.01). **(B)** Cells seeded in 12-well plates were infected with SVCV at MOI 0.003. At indicated time points, cells were trypsinized and collected for trypan blue staining. Error bars represent the standard error of the mean (+SEM) of three independent experiments. **(C)** Cells seeded in 12-well plates were infected with SVCV as in (B). The culture supernatants were collected at indicated time points for viral titer determination as in (A). **(D)** Cells in 12-well plates were infected with SVCV (MOI 0.003) at various time points. RNA was extracted and SVCV-N transcript was analyzed by qPCR. β-actin was used as an internal control for normalization. The relative expression level of SVCV-N was normalized against the expression level in cells at 2 h post infection. **(E ~ H)** qPCR detection of IFNa, PKR, Viperin and Mx1 mRNA level in 2nFC, 3nFC and 4nFC. Cells seeded in 12-well plates were infected with SVCV (MOI 0.003). Samples were collected for RNA extraction at 0 h, 2 h, 4 h and 24 h post infection. β-actin was used as an internal control for normalization, and the relative expression is represented as the fold induction relative to the expression level in the cells without infection (0 h). Error bars represent + SD of three independent experiments (*p < 0.05; **p < 0.01). 2n:2nFC; 3n:3nFC; 4n:4nFC.

Table 2
Summary of the Illumina HiSeqTM 2500 sequencing output for all samples.

Sample	Clean reads	Clean bases	Valid ratio (base)	Q30 (%)	GC content (%)
2N CTR	41992154	5249019250	99.98%	96.71%	50.10%
2N SVCV	37219618	4652452250	99.98%	96.72%	51.35%
3N CTR	47992506	5999063250	99.98%	96.84%	50.82%
3N SVCV	25934388	3241798500	99.98%	96.90%	46.51%
4N CTR	47992746	5999093250	99.98%	96.80%	50.64%
4N SVCV	32388210	4048526250	99.98%	96.25%	47.47%

Table 3
Statistics of assembled result.

	2N Unigenes	3N Unigenes	4N Unigenes
Number	41179	40547	40385
> =500 bp	23994	22191	22583
> =1000 bp	13368	10786	11937
N50	1936	1293	1555
Total Length	46087950	36144592	39443329
Max Length	16466	14083	14663
Min Length	301	301	301
Average Length	1119.21	891.42	976.68

against viral infection, it is speculated that the different innate immune response level or/and mechanism may lead to the different antiviral abilities of these fishes with different ploidy. For this reason, we investigated the variation of innate immune related pathway of 2nFC, 3nFC and 4nFC in response to SVCV infection. Based on the KEGG classification, RIG-I like receptor signaling pathway, Cytosolic DNA-sensing pathway, Toll-like receptor signaling pathway were clearly activated in 2nFC and 3nFC (Fig. 5D&E). While in 4nFC, Toll-like receptor signaling pathway and NOD-like receptor signaling pathway were activated evidently (Fig. 5F). This information of innate immune related pathways will be useful for us to explore and understand the innate immune systems of red crucian carp, triploid hybrid and allotetraploid fish.

To validate the veracity and reliability of the transcriptome data, seven innate immune related genes were selected and investigated by qPCR, which including RIG-I, MDA5, LGP2, MAVS, TBK1, TRAF6 and IRF7. The qPCR results revealed parallel expression affinity with the RNA-seq data, with the exception of some quantitative differences at the expression level (Fig. 6). Thus the qPCR results were significantly co-related with the RNA-seq expression, indicating the reliability of RNA-seq data.

4. Discussion

It is reported that fish teleost fishes with different ploidy presented varied immune activities. The studies on Ayu (*Plecoglossus altivelis*) and Atlantic salmon (*Salmo salar*) showed that diploid and triploid fish owned similar resistance to infectious diseases (Chalmers et al., 2017; Inada Y and Taniguchi, 1990). However, reports about Amazon molly (*Poecilia formosa*) and Chinook salmon (*Oncorhynchus tshawytscha*) showed that triploid fish had stronger resistance to pathogen invasion than diploid fish (Ching et al., 2010; Lampert et al., 2009). Distant hybridization can combine the genomes of different species, which leads to the changes of the offspring in phenotypes and genotypes. By this strategy, triploid and allotetraploid have been successfully developed in this lab. It has been observed that triploid fish display much improved disease resistance than its parents (Liu, 2010). This suggests that triploid hybrid might possess “improved” innate immune mechanism compared with its parents–red crucian carp and allotetraploid fish. It is speculated that erroneous DNA excision between homologous

Table 4
Statistics of functional annotation of unigenes.

Database	2N		3N		4N	
	Number	Percentage	Number	Percentage	Number	Percentage
NR	30111	73.12%	31164	76.86%	30163	74.69%
SWISSPROT	20492	49.76%	21811	53.79%	20673	51.19%
KOG	16387	39.79%	17335	42.75%	16339	40.46%
KEGG	8442	20.50%	9063	22.35%	8369	20.72%
GO	18676	45.35%	19914	49.11%	18920	46.85%

parental genes may drive the high percentage of chimeric genes, or even more potential mechanisms may result in this phenomenon (Liu et al., 2016).

In the current work, three new caudal fin cell lines from diploid red crucian carp, triploid hybrid and allotetraploid have been established separately, which show fibroblast-like morphology. It is reported that the cell types of teleost fin *in vitro* is very complex. Fin is mainly composed of epidermis (containing epithelial cells) and dermis (containing fibroblasts). Therefore only by cell morphology cannot predict

Table 5
Statistics of differentially expressed unigene.

Sample	Up regulated	Down regulated	Total
2N SVCV vs. 2N CTR	1485	675	2160
3N SVCV vs. 3N CTR	359	43	402
4N SVCV vs. 4N CTR	683	402	1085

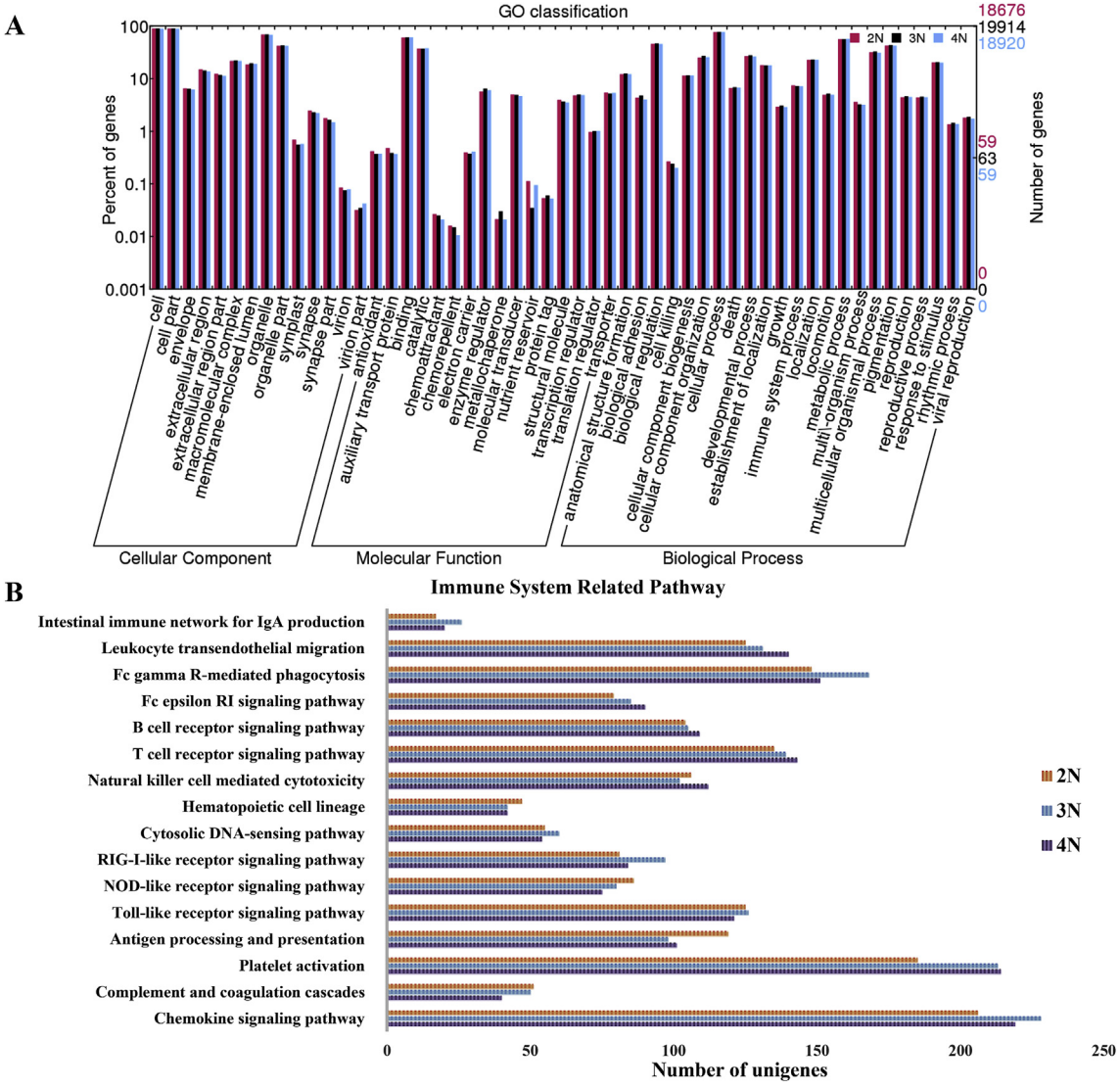

Fig. 4. GO and KEGG classification of assembled unigenes. **(A)** All the annotated transcripts were grouped into three categories after GO classification: cellular component, molecular function and biological process. The Y-axis indicated the number of genes in each category, the X-axis represent various gene function. **(B)** The numbers of assembled unigenes enriched in immune system related pathways by KEGG annotation. The X-axis corresponds to the numbers of unigenes and the Y-axis represents different pathway. 2N:2nFC; 3N:3nFC; 4N:4nFC.

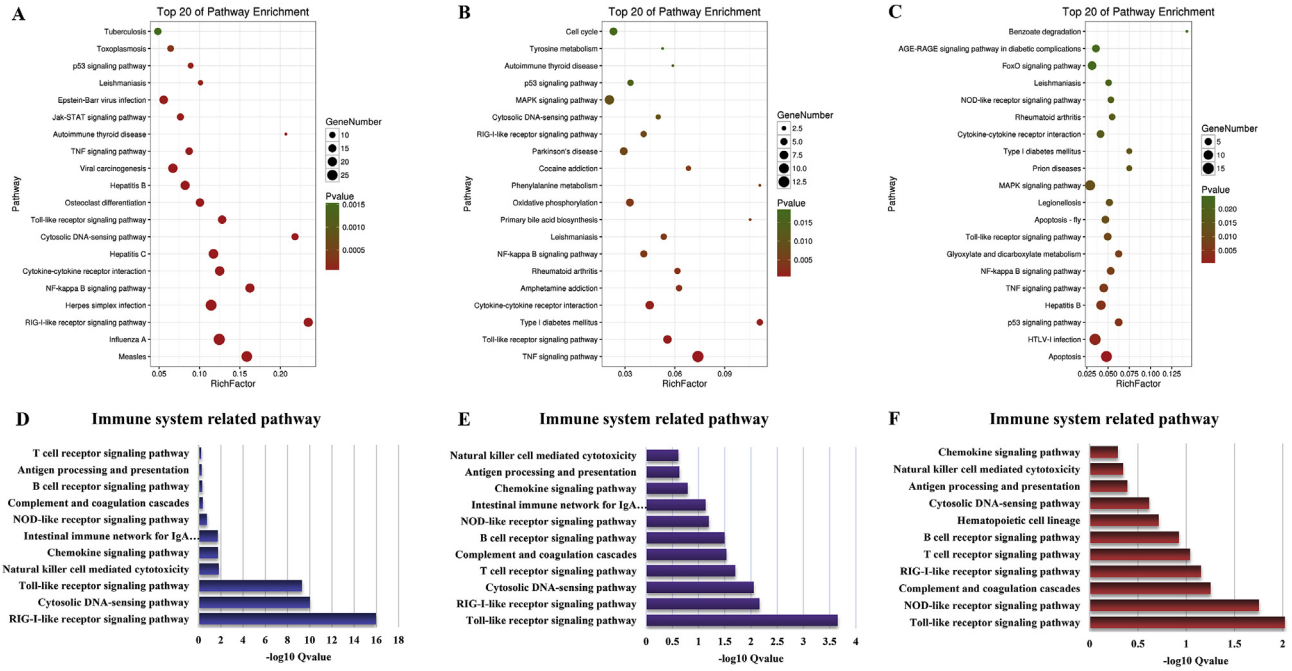

Fig. 5. Top 20 statistics of pathway enrichment based on the DEGs after SVCV infection and immune system related pathway enrichment statistics. **(A–C)** Scatter plot of KEGG pathway enrichment statistics after SVCV infection in 2nFC (A), 3nFC (B) and 4nFC (C). RichFactor is the ratio of DEG numbers noted in this pathway term to all gene numbers noted in this pathway term. The X-axis corresponds to rich factor of pathway, and the Y-axis represents different pathway. The magnitude of the pots displays gene number, and p-value is described by the color classification. **(D–F)**: The immune system related pathways enrichment analysis of DEGs of 2nFC (D), 3nFC (E) and 4nFC (F). (For interpretation of the references to color in this figure legend, the reader is referred to the Web version of this article.)

the tissue origin of cultured fin cells precisely (Mauger et al., 2009). *ck49* and *col1a1* have been reported as marker genes to identify the cell phenotype of fin cells (Chenais et al., 2015). Our study revealed that a low ck49 (epithelial marker) and a high *col1a1* (dermis marker) expression level were detected in 2nFC, 3nFC and 4nFC, respectively (Fig. 1B). These results suggest that 2nFC, 3nFC and 4nFC are fibroblastic cells. It was interesting that the growth rate of these cell lines correlated with the ploidy of their donors in that the growth rate decreased as the DNA content or the chromosome number of the donors increased (Fig. 1C).

It is reported that fish fins constitute a major entry point of virus and fibroblast-like fin cell line derived from rainbow trout was a suitable model to investigate their antiviral mechanisms against rhabdovirus VSHV infection (Cornwell et al., 2013; Grady et al., 2011; Montero et al., 2011; Quillet et al., 2001, 2007; Verrier et al., 2012, 2013; Vo et al., 2016). For cyprinid fish species, SVCV is a negative-sense ssRNA virus belongs to rhabdoviridae and causes serious haemorrhagic disease. Therefore, in this work, we decided to study whether 2nFC, 3nFC and 4nFC were good models for studying their immune gene expression and antiviral mechanisms in rhabdovirus infection. The viral infection experiment results demonstrated that 2nFC, 3nFC and 4nFC were capable of supporting the replication of the rhabdovirus SVCV. In addition, the virus titer produced in 3nFC was much lower than that in 2nFC and 3nFC and also the mortality of 3nFC after infection was the lowest (Fig. 3A ~ C), indicating that 3nFC possesses the strongest viral resistance to SVCV. Furthermore, we detected a lowest SVCV-N mRNA expression level in 3nFC and a highest level in 4nFC, which is consistent with the viral titer of their supernatants (Fig. 3D). These observations suggest that the antiviral ability of 3nFC might be potently activated to inhibit the replication of SVCV.

In teleost, type I IFNs signaling system played a crucial role in the host antiviral activity. After the invasion of virus, IFNs are able to induce a large diversity of antiviral ISGs, which encode cytokines and antiviral proteins. We therefore investigated the induction of IFN and ISGs in 2nFC, 3nFC and 4nFC at different time points post SVCV infection (Fig. 3E ~ H). It was found that the mRNA level of IFN and ISGs in 2nFC and 3nFC raised at 24 h post infection. In contrast, we were not able to detect a significantly increase of IFN or ISGs expression level in 4nFC post viral infection. These data imply that the IFN system of 3nFC and 2nFC were more sensitive and intensive than that of 4nFC. To

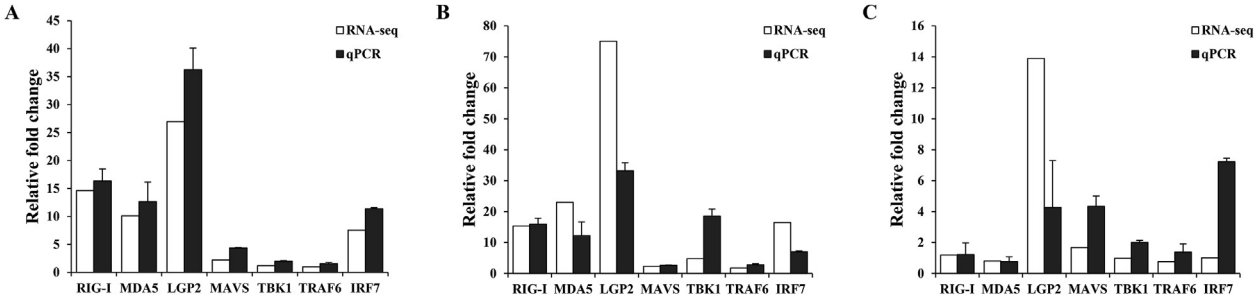

Fig. 6. qPCR for validation of RNA-seq. The expressions of several innate immune related genes of 2nFC, 3nFC and 4nFC, such as RIG-I, MDA5, LGP2, MAVS, TBK1, IRF7 and TRAF6 were detected by RNA-seq (white column) and qPCR (black column). **(A)**: validation of innate immune related genes of 2nFC; **(B)**: validation of innate immune related genes of 3nFC; **(C)**: validation of innate immune related genes of 4nFC.

further check the function of IFN system of the cell lines, the cells were pretreat with poly I:C 24 h before SVCV infection (Supplementary Fig. 1). It was observed that the pretreatment of the cell lines with poly I:C delayed the cell death to SVCV infection except 4nFC. Taken together, these results suggest that the IFN system of 3nFC and 2nFC were more sensitive and intensive than that of 4nFC.

In order to get a comprehensive understanding of the antiviral response and innate immune mechanism of 2nFC, 3nFC and 4nFC to SVCV infection, we employed the RNA-seq technology to investigate the transcriptome of these cell lines. In the transcriptome data, more than 40000 unigenes were separately acquired after assembling and filtration in 2nFC, 3nFC and 4nFC. The GO annotation and KEGG pathway annotation of unigenes showed that these cell lines contain abundant immune related genes (Fig. 4A&B). This suggested that the basic components and signaling pathways necessary for innate and adaptive immunity exist in 2nFC, 3nFC and 4nFC. In the context of viral infection, the virus-specific component could detected by host pattern-recognition receptors (PRRs), including Toll-like receptors (TLRs), RIG-I like receptors (RLRs) and NOD-like receptors (NLRs), which initiate antiviral response such as the induction of type I IFN and ISGs (Chen et al., 2017; Zou and Secombes, 2011). KEGG pathway enrichment analysis showed that most of the top 20 pathways enriched in 2nFC, 3nFC and 4nFC were immune-related and disease-related pathways, which indicated that the immune response was the most important changes in response to SVCV infection (Fig. 5A ~ C). In 2nFC and 3nFC, RLR signaling pathway, TLR signaling pathway and cytosolic DNA-sensing pathway were activated remarkably, which were major signaling pathways response against viral infection. Interestingly, in 4nFC, RLR signaling pathway was not involved in top 20 statistics of pathway enrichment. Consistent with this point, the upregulation of RIG-I, MDA5 and LGP2 in 2nFC and 3nFC were much higher than those in 4nFC (Fig. 6). Taken together, conclusions could be draw from our results that 3nFC had strongest antiviral ability depends on its fast and robust activation of RLR/TLR/IFN signaling pathway. Aquaculture experience demonstrates that allotetraploid fish are more susceptible to SVCV than red crucian carp and triploid hybrid (Liu, 2010). Multiple mechanisms might have been involved in that 4nFC appeared to be more SVCV-susceptible. It is speculated that a weaker response to activate RLR signaling pathway and its downstream IFN signaling pathway in 4nFC, which results in a higher viral titer in 4nFC and mortality of 4nFC post SVCV infection.

Acknowledgements

This work was supported by National Natural Science Foundation of China (81471963, 31272634) and China Postdoctoral Science Foundation (2018M632970).

Appendix A. Supplementary data

Supplementary data related to this article can be found at https://doi.org/10.1016/j.dci.2018.07.007.

References

Chalmers, L., Taylor, J., Roy, W., Preston, A., Migaud, H., Adams, A., 2017. A comparison of disease susceptibility and innate immune response between diploid and triploid Atlantic salmon (*Salmo salar*) siblings following experimental infection with Neoparamoeba perurans, causative agent of amoebic gill disease. Parasitology 144, 1229–1242.

Chen, S., Zou, P., Nie, P., 2017. Retinoic acid-inducible gene I (RIG-I)-like receptors (RLRs) in fish: current knowledge and future perspectives. Immunology 151, 16–25.

Chen, S., Wang, J., Liu, S., Qin, Q., Xiao, J., Duan, W., Luo, K., Liu, J., Liu, Y., 2009. Biological characteristics of an improved triploid crucian carp. Sci. China Ser. C Life Sci. 52, 733–738.

Chenais, N., Lareyre, J.J., Le Bail, P.Y., Labbe, C., 2015. Stabilization of gene expression and cell morphology after explant recycling during fin explant culture in goldfish. Exp. Cell Res. 335, 23–38.

Ching, B., Jamieson, S., Heath, J.W., Heath, D., Hubberstey, A., 2010. Transcriptional differences between triploid and diploid Chinook salmon (*Oncorhynchus tshawytscha*) during live Vibrio anguillarum challenge. Heredity 104, 224–234.

Cornwell, E.R., Bellmund, C.A., Groocock, G.H., Wong, P.T., Hambury, K.L., Getchell, R.G., Bowser, P.R., 2013. Fin and gill biopsies are effective nonlethal samples for detection of Viral hemorrhagic septicemia virus genotype IVb. J. Vet. Diagn. Invest. 25, 203–209.

Driever, W.R., 1993. Characterization of a cell line derived from zebrafish (*brachydanio rerio*) embryos. Vitro Anim. Cell Dev. Biol. 29, 749.

Duan, W., Xu, K., Hu, F., Zhang, Y., Wen, M., Wang, J., Tao, M., Luo, K., Zhao, R., Qin, Q., Zhang, C., Liu, J., Liu, Y., Liu, S., 2016. Comparative proteomic, physiological, morphological, and biochemical analyses reveal the characteristics of the diploid spermatozoa of allotetraploid hybrids of red crucian carp (*Carassius auratus*) and common carp (*Cyprinus carpio*). Biol. Reprod. 94, 35.

Grady, C.A., Gregg, J.L., Wade, R.M., Winton, J.R., Hershberger, P.K., 2011. Viral replication in excised fin tissues (VREFT) corresponds with prior exposure of Pacific herring, Clupea pallasii (Valenciennes), to viral haemorrhagic septicaemia virus (VHSV). J. Fish. Dis. 34, 3–12.

Inada Y, Y., Taniguchi, N., 1990. Study on the resistance to vibriosis in induced triploid ayu Plecoglossus altivelis. Bull. Jpn. Soc. Sci. Fish. 56, 1587–1591.

Ingerslev, H., Ossum, C., Lindenstrom, T., Nielsen, M., 2010. Fibroblasts express immune relevant genes and are important sentinel cells during tissue damage in rainbow trout (*Oncorhynchus mykiss*). PLoS One 5, e9304.

Lakra, W., Swaminathan, T., Joy, K., 2011. Development, characterization, conservation and storage of fish cell lines: a review. Fish Physiol. Biochem. 37, 1–20.

Lampert, K., Fischer, P., Schartl, M., 2009. Major histocompatibility complex variability in the clonal Amazon molly, Poecilia formosa: is copy number less important than genotype? Mol. Ecol. 18, 1124–1136.

Liu, J., Li, J., Xiao, J., Chen, H., Lu, L., Wang, X., Tian, Y., Feng, H., 2017. The antiviral signaling mediated by black carp MDA5 is positively regulated by LGP2. Fish Shellfish Immunol. 66, 360–371.

Liu, S., 2010. Distant hybridization leads to different ploidy fishes. Science China. Life Sci. 53, 416–425.

Liu, S., Liu, Y., Zhou, G., Zhang, X., Luo, C., Feng, H., He, X., Zhu, G., Yang, H., 2001. The formation of tetraploid stocks of red crucian carp × common carp hybrids as an effect of interspecific hybridization. Aquaculture 192, 171–186.

Liu, S., Luo, J., Chai, J., Ren, L., Zhou, Y., Huang, F., Liu, X., Chen, Y., Zhang, C., Tao, M., Lu, B., Zhou, W., Lin, G., Mai, C., Yuan, S., Wang, J., Li, T., Qin, Q., Feng, H., Luo, K., Xiao, J., Zhong, H., Zhao, R., Duan, W., Song, Z., Wang, Y., Wang, J., Zhong, L., Wang, L., Ding, Z., Du, Z., Lu, X., Gao, Y., Murphy, R.W., Liu, Y., Meyer, A., Zhang, Y.P., 2016. Genomic incompatibilities in the diploid and tetraploid offspring of the goldfish × common carp cross. Proc. Natl. Acad. Sci. U.S.A. 113, 1327–1332.

Liu, S.J., Sun, Y.D., Zhang, C., Luo, K.K., Liu, Y., 2004. Triploid crucain carp-allotetraploid hybrids (male) × goldfish (hermaphrodite). Acta Genetica Sin. 31, 31–38.

Long, Y., Liu, S., Huang, W., Zhang, J., Sun, Y., Zhang, C., Chen, S., Liu, J., Liu, Y., 2006. Comparative studies on histological and ultra-structure of the pituitary of different ploidy level fishes. Sci. China Ser. C Life Sci. 49, 446–453.

Luque, A., Gonzalez Granja, A., Gonzalez, L., Tafalla, C., 2014. Establishment and characterization of a rainbow trout heart endothelial cell line with susceptibility to viral hemorrhagic septicemia virus (VHSV). Fish Shellfish Immunol. 38, 255–264.

Mable, B.K., 2004. 'Why polyploidy is rarer in animals than in plants': myths and mechanisms. Biol. J. Linn. Soc. 82, 453–466.

Mable, B.K., 2013. Polyploids and hybrids in changing environments: winners or losers in the struggle for adaptation? Heredity 110, 95–96.

Mauger, P.E., Labbé, C., Bobe, J., Cauty, C., Leguen, I., Baffet, G., Le Bail, P.Y., 2009. Characterization of goldfish fin cells in culture: some evidence of an epithelial cell profile. Comp. Biochem. Physiol. B Biochem. Mol. Biol. 152, 205–215.

Montero, J., Garcia, J., Ordas, M.C., Casanova, I., Gonzalez, A., Villena, A., Coll, J., Tafalla, C., 2011. Specific regulation of the chemokine response to viral hemorrhagic septicemia virus at the entry site. J. Virol. 85, 4046–4056.

Morozova, O., Marra, M., 2008. Applications of next-generation sequencing technologies in functional genomics. Genomics 92, 255–264.

Petit, J., David, L., Dirks, R., Wiegertjes, G., 2017. Genomic and transcriptomic approaches to study immunology in cyprinids: what is next? Dev. Comp. Immunol. 75, 48–62.

Qin, Q., Wu, T., Jia, T., Hegde, A., Zhang, R., 2006. Development and characterization of a new tropical marine fish cell line from grouper, Epinephelus coioides susceptible to iridovirus and nodavirus. J. Virol Meth. 131, 58–64.

Quillet, E., Dorson, M., Aubard, G., Torhy, C., 2001. In vitro viral haemorrhagic septicaemia virus replication in excised fins of rainbow trout correlation with resistance to waterborne challenge and genetic variation. Dis. Aquat. Org. 45, 171–182.

Quillet, E., Dorson, M., Aubard, G., Torhy, C., 2007. In vitro assay to select rainbow trout with variable resistance susceptibility to viral haemorrhagic septicaemia virus. Dis. Aquat. Org. 76, 7–16.

Shen, J., Liu, S., Sun, Y., Zhang, C., Luo, K., Tao, M., Zeng, C., Liu, Y., 2006. A new type of triploid crucian crap–red crucian crap (♀) × allotetraploid (♂). Prog. Nat. Scie.: Mater. Int. 16, 1348–1352.

Verrier, E.R., Dorson, M., Mauger, S., Torhy, C., Ciobotaru, C., Hervet, C., Dechamp, N., Genet, C., Boudinot, P., Quillet, E., 2013. Resistance to a rhabdovirus (VHSV) in rainbow trout: identification of a major QTL related to innate mechanisms. PLoS One 8, e55302.

Verrier, E.R., Langevin, C., Tohry, C., Houel, A., Ducrocq, V., Benmansour, A., Quillet, E., Boudinot, P., 2012. Genetic resistance to rhabdovirus infection in teleost fish is paralleled to the derived cell resistance status. PLoS One 7, e33935.

Villena, A., 2003. Applications and needs of fish and shellfish cell culture for disease control in aquaculture. Rev. Fish Biol. Fish. 13, 111–140.

Vo, N.T., Bender, A.W., Lumsden, J.S., Dixon, B., Bols, N.C., 2016. Differential viral

haemorrhagic septicaemia virus genotype IVb infection in fin fibroblast and epithelial cell lines from walleye, Sander vitreus (Mitchill), at cold temperatures. J. Fish. Dis. 39, 175–188.
Wu, H., Liu, L., Wu, S., Wang, C., Feng, C., Xiao, J., Feng, H., 2017. IFNb of black carp functions importantly in host innate immune response as an antiviral cytokine. Fish Shellfish Immunol. 74, 1–9.
Xiao, J., Kang, X.W., Xie, L.H., Qin, Q.B., He, Z.L., Hu, F.Z., Zhang, C., Zhao, R.R., Wang, J., Luo, K.K., Liu, Y., Liu, S.J., 2014. The fertility of the hybrid lineage derived from female *Megalobrama amblycephala* × male *Culter alburnus*. Anim. Reprod. Sci. 151, 65–70.
Xiao, J., Yan, C., Zhou, W., Li, J., Wu, H., Chen, T., Feng, H., 2017. CARD and TM of MAVS of black carp play the key role in its self-association and antiviral ability. Fish Shellfish Immunol. 63, 261–269.
Xue, T., Wang, Y., Pan, Q., Wang, Q., Yuan, J., Chen, T., 2018. Establishment of a cell line from the kidney of black carp and its susceptibility to spring viremia of carp virus. J. Fish. Dis. 41, 365–374.
Yan, J., Peng, L., Li, Y., Fan, H., Tian, Y., Liu, S., Feng, H., 2016. IFNa of triploid hybrid of gold fish and allotetraploid is an antiviral cytokine against SVCV and GCRV. Fish Shellfish Immunol. 54, 529–536.
Zhang, C., He, X., Liu, S., Sun, Y., Liu, Y., 2005. Chromosome pairing in meiosis I in allotetraploid hybrids and allotriploid crucian carp. Acta Zool. Sin. 51, 89–94.
Zhang, Q., Ruan, H., Li, Z., Yuan, X., Gui, J., 2003. Infection and propagation of lymphocystis virus isolated from the cultured flounder Paralichthys olivaceus in grass carp cell lines. Dis. Aquat. Org. 57, 27–34.
Zhang, Y., Gui, J., 2004. Molecular characterization and IFN signal pathway analysis of Carassius auratus CaSTAT1 identified from the cultured cells in response to virus infection. Dev. Comp. Immunol. 28, 211–227.
Zou, J., Secombes, C.J., 2011. Teleost fish interferons and their role in immunity. Dev. Comp. Immunol. 35, 1376–1387.
Zuo, W., Qian, H., Xu, Y., Du, S., 1986. A cell line derived from the kidney of grass carp (*Ctenopharyngodon idellus*). J. Fish. China 10, 11–17.